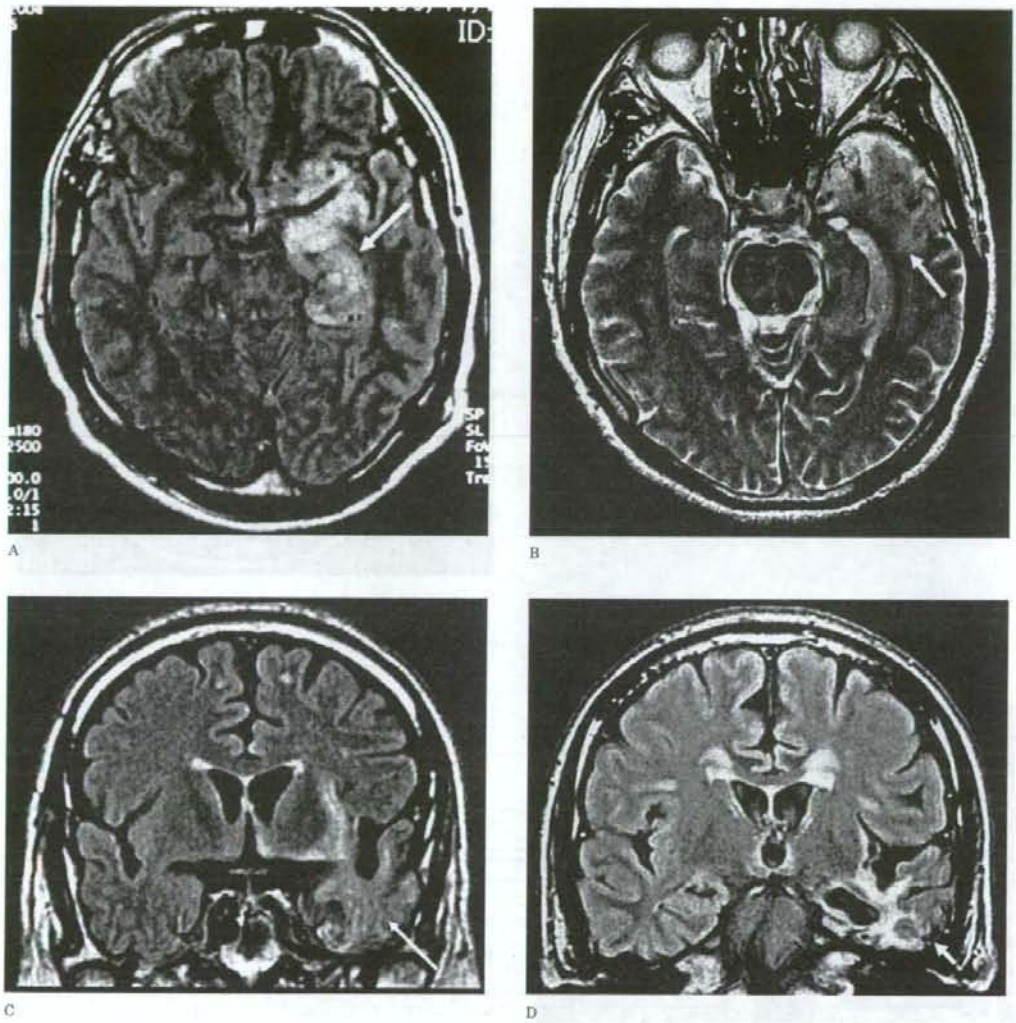

Figure 1 A-D A 54-year-old-male with HSE. A) FLAIR image at 2 days after onset shows hyperintensity with swelling in the left medial temporal cortices (white arrow). B) T2 weighted image at 3 weeks after onset shows hyperintensity in the left anterior temporal white matter (white arrow) and cortices. C) FLAIR coronal image at 3 weeks after onset demonstrates hyperintensity in the left temporal white matter (white arrow), left extreme capsule and claustrum (black arrowhead). D) FLAIR coronal image at 22 months after onset demonstrates that hyperintensiy in the left temporal white matter decreased in size with white matter volume loss. The medial temporal cortex showed severe damage with atrophy.

to indicate that immune activation is involved in the pathogenesis of HSE relapse. They suggested that these CSF findings, which indicate immunologically mediated pathogenesis, served as surrogate markers for HSE relapse. Unfortunately, in our analysis, CSF markers such as CD8 and IFN-γ were not examined, but we had sufficient follow-up imaging studies which were absent in their study; No obvious CT abnormalities were observed. MRI was performed

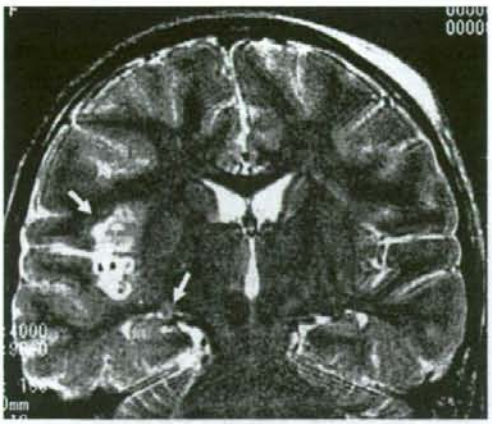

A

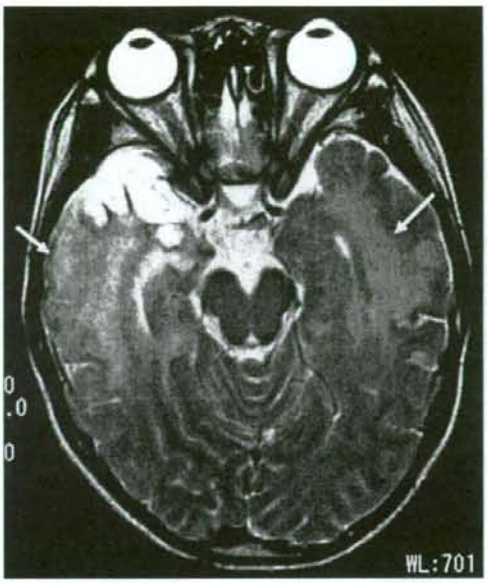

B

C

Figure 2 A-C A 10-year-old female with HSE. A) 3 days after onset. T2 weighted coronal image showed hyperintensity in the right hippocampus, parahippocampal gyri, right insula with swelling. Left parietal region of the scalp shows subcutaneous swelling and hyperintensity probably representing incidental hematoma. B) 3 weeks after onset. T2 weighted axial image shows hyperintensity in the bilateral temporal (white arrow) white matter. Right medial temporal cortices already show obvious atrophic change. C) 22 months after onset. Hyperintensity lesions in the bilateral temporal white matter improve.

in the fourth month after the start of symptoms in only one case, and there was a note saying "T2 gliosis oedema?" It would be interesting to see whether these findings corresponded to the white matter lesions we noted.

Persistence or recurrence (or reactivation) and/or immunologically mediated demyelinization of the brain tissue of HSV have been implicated in the pathogenesis of HSE relapse. The reason our cases showed a rise in white

Table 2 Distribution of the white matter lesions associated with HSE in subacute to chronic stage *GM*: gray matter, *WM*: white matter, *T*: temporal lobe, *dT*: deep temporal lobe including hippocampus, *F*: frontal lobe.

Case No	*Affected site in acute phase*		*Affected site in subacute to chronic stages*		*Spontaneous subsidence of white matter lesions*
	GM	*WM*	*GM*	*WM*	
1	Lt T, dT	–	Atrophy in lt T, dT	Lt T	+
2	Rt T, dT	–	Atrophy in rt T, dT	Bil T Rt F	+
3	Bil T, dT	–	Atrophy in bil T, dT	Bil T Bil F	+
4	Let T,dT	–	Atrophy in lt T,dT	Bil T Lt F	+
5	Rt T, dT	–	Atrophy in rt T, dT	Bil T Rt F	+
6	Bil T, dT	–	Atrophy in Bil T, dT	Bil T Bil F	+

matter signals is not clear at present, but it is difficult to rule out the possibility of subclinical relapse. After infection with HSE, each white matter signal change occurring in the subacute stage was self-limiting and was accompanied by white matter atrophy in the chronic stage. Thus, we should consider the possibility that the process is immune-mediated. It is possible that MRI examination, which is noninvasive and may be performed repeatedly, can play a role as a more precise surrogate marker flanked by other data, such as CSF findings showing immune-mediated abnormalities.

De Tiege et Al reported a case of a three-year-old male infant who showed secondary acute neurological deterioration one month after HSE onset[5]. In this case, diffuse signal rises were seen on FLAIR in the right temporal lobe white matter on MRI performed on the 44th day after HSE infection and on the 12th day after secondary acute neurological deterioration. Incomplete regression of white matter lesions, as well as contraction, were seen on the follow-up MRI performed three and a half years later, which was similar to our image progression. Though they also lacked biological evidence, except for the clinical and image changes, based on the notion that corticosteroid treatment had clinical utility against secondary acute neurological deterioration, they suggested the possibility of postinfectious immune-mediated encephalitis after pediatric HSE. It is difficult to identify obvious differences between our studies at present, except for the fact that De Tiege et Al's report was pediatric. Through analysis of further cases, it will be possible to clarify the reasons for the clinical exacerbation occurring in their case, but not in the present six cases.

It is known that HSE accompanies chronic granulomatous encephalitis, and chronic in-

flammation and gliosis with extensive mineralization of brain tissue were pathologically demonstrated [6,7]. Although the clinical course in those cases showed progressive neurological deficits and intractable seizures, unlike our white matter abnormality cases, it is desirable to investigate image progression and whether pathogenesis in the two studies were intrinsically different.

White matter lesions in the chronic phase of HSE have been reported in an experimental mouse study [8]. Although mice clinically recovered from two weeks after infection and brain viral load decreased, neuropathological and MRI findings remained at six months. Meyding-Lamade et Al thus hypothesized that these changes were due to secondary immune-mediated tissue damage, rather than direct virus-mediated mechanisms [6]. This animal model is important in the discussion of underlying white matter lesions. However, the report did not discuss the involvement of the white matter in these lesions [6]. Tamura et Al described a patient who tested positive for myelin basic protein (MBP). This may reflect demyelination, which should be investigated in more patients in the future [3]. Imaging studies of a cohort of patients surviving PCR-confirmed HSE are also needed to determine whether this pattern is occasional or represents a common form of progression. No significant differences in neurological findings, CSF data or acyclovir dose were noted between patients with and without signal abnormalities in white matter. We were therefore unable to identify the conditions leading to white matter signal abnormalities. Further investigations are necessary.

Conclusions

On long-term observation of HSE, signal abnormalities in the white matter often occur during the subacute stage and can persist for long periods of time. Although the mechanisms underlying these white matter lesions have not been elucidated, subclinical immune-mediated relapse may be considered.

References

1 Ueda N, Miyasaki H, Kuroiwa Y: Diffuse white matter lesions in a case of herpes simplex encephalitis. J Neurol 250: 867-868, 2003.
2 Mitsufuji N, Ikuta H: Asymptomatic self-limiting white matter lesions in the chronic phase of herpes simplex encephalitis. Brain Dev 24: 300-303, 2002.
3 Tamura T, Morikawa A, Kikuchi K: Diffuse white matter lesions associated with herpes simplex encephalitis as observed on magnetic resonance imaging. Brain Dev 18:150-152, 1996.
4 Sköldenberg B, Aurelius E, Hjalmarsson A, Sabri F, Forsgren M, Andersson B et Al: Incidence and pathogenesis of clinical relapse after herpes simplex encephalitis in adults. J Neurol 253: 163-170, 2006.
5 De Tiege X, De laet C, Mazoin N et Al: Postinfectious immune-mediated encephalitis after pediatric herpes simplex encephalitis. Brain & Development 27: 304-307, 2005.
6 Prats Vinas JM, Martinez Gonzalez MJ, Garcia Rives A et Al: Postencephalitic chronic granulomatous disease. Pediatr Neurol 35: 297-299, 2006.
7 Love S, Koch P, Urbach H et Al: Chronic granulomatous herpes simplex encephalitis in children. J Neuropathol Exp Neurol 63: 1173-1181, 2004.
8 Meyding-Lamadé U, Lamadé W, Kehm R et Al: Herpes simplex virus encephalitis: chronic progressive cerebral MRI changes despite good clinical recovery and low viral load-an experimental mouse study. European Journal of Neurology 6: 531-538, 1999.

Aya Midori Tokumaru, MD
Department of Radiology
Tokyo Metropolitan Medical Center of Gerontology
35-2 Sakae-Cho Itabashi-Ku
173-0015 Tokyo, JAPAN
Tel.: 81-3-3964-1141
Fax: 81-3-3964-1982
E-mail: tokumaru@tmgh.metro.tokyo.jp

CE: Satish ED: Prabhu Op: Jay WNR: LWW.WNR.4299

NEUROREPORT

Presynaptic and postsynaptic nigrostriatal dopaminergic functions in multiple system atrophy

Masaya Hashimoto[a,c], Keiichi Kawasaki[a], Masahiko Suzuki[a,c], Kazuko Mitani[a,d], Shigeo Murayama[b], Masahiro Mishina[a,e], Keiichi Oda[a], Yuichi Kimura[a], Kiichi Ishiwata[a], Kenji Ishii[a] and Kiyoharu Inoue[c]

[a]Positron Medical Center, [b]Department of Neuropathology, Tokyo Metropolitan Institute of Gerontology, [c]Department of Neurology, Jikei University School of Medicine, [d]Department of Neurology, Tokyo Metropolitan Geriatric Hospital, Tokyo and [e]Neurological Institute, Nippon Medical School Chiba Hokusoh Hospital, Chiba, Japan

Correspondence to Kenji Ishii, Positron Medical Center, Tokyo Metropolitan Institute of Gerontology, 1-1 Naka-cho, Itabashi-ku, Tokyo 173-0022, Japan

Tel: +81 3 3964 3241 EX3503; fax: +81 3 3964 2188; e-mail: ishii@pet.tmig.or.jp

Received 7 September 2007; accepted 30 October 2007

A simultaneous evaluation of presynaptic and postsynaptic dopaminergic positron emission tomography markers, the dopamine transporters and the dopamine D_2-like receptors, was performed in eight patients with parkinsonian phenotype of multiple system atrophy. Both presynaptic and postsynaptic markers were revealed to have declined in such a manner that they kept strong positive correlation throughout the striatum of all patients, suggesting that the degeneration process in the striatum may involve the entire structure of the dopaminergic synapse. In two L-3,4,dihydroxyphenyl-alanine-responsive cases, the balance of decline in two markers was relatively shifted to presynaptic dominant side. Correlative positron emission tomography study of presynaptic and postsynaptic dopaminergic function may be useful for the diagnosis of multiple system atrophy and to understand the mechanisms of its temporal L-3,4,dihydroxyphenyl-alanine responsiveness. *NeuroReport* 00:000–000 © 2008 Wolters Kluwer Health | Lippincott Williams & Wilkins.

Keywords: dopamine receptor, dopamine transporter, L-3,4,dihydroxyphenyl-alanine responsiveness, multiple system atrophy, Parkinson, positron emission tomography

Introduction

In patients with the parkinsonian phenotype of multiple system atrophy (MSA-P), a pathological abnormality is observed mainly in the substantia nigra (SN), striatum, ceruleus nucleus, pontine nuclei, inferior olivary nucleus, cerebellum, and spinal cord. The impairment is particularly severe in the SN and striatum [1], and neuronal loss and gliosis are the features of the pathology [2]. Neuroimaging studies using positron emission tomography (PET) [3] and single photon emission computed tomography techniques [4] have reported reduced glucose metabolism in the striatum and declined nigrostriatal dopaminergic neural transmission function in both the presynaptic and postsynaptic sites. No pathological or neuroimaging studies, however, have examined the relationship between the degeneration/dysfunction of nigrostriatal presynaptic and postsynaptic dopaminergic systems. It is well known that responses to L-3,4,dihydroxyphenyl-alanine (L-DOPA) are generally poor in MSA [1], and this is ascribable to the fact that the pathology of MSA involves not only SN but also the striatum where the dopamine receptors exist. A transient effect, however, is occasionally noted in the early stages in certain cases. Wenning *et al.* [5] proposed a hypothesis based on the pathological finding of a dissociation between the SN and striatal degeneration that may account for such L-DOPA responsiveness. No pathological or neuroimaging evidence that directly demonstrated the dissociation in such cases, however, has been found.

We simultaneously measured the presynaptic and postsynaptic nigrostriatal dopaminergic functions using PET in MSA-P patients, including L-DOPA-responsive cases, and the regional correlation of two parameters was analyzed in the striatum to examine the characteristics of the disease and the mechanisms of L-DOPA responsiveness.

Methods

This study was approved by the Ethical Committee of Tokyo Metropolitan Institute of Gerontology. The objective and effect of the PET examination on the human body were adequately explained to all participants, and written informed consent was obtained.

Participants

We studied eight patients (68.9 ± 7.4 years old) clinically diagnosed as MSA-P according to the consensus criteria established by Gilman *et al.* [6] (Table 1). The MSA-P patients underwent PET examination following a 15-h deprivation of antiparkinsonian drugs. The primary symptom observed in all the patients was parkinsonism; further, during the course of the disease, parkinsonism was noted to be the cardinal symptom. Magnetic resonance imaging

Table 1 Clinical features of the eight patients with the parkinsonian phenotype of multiple system atrophy

Patient no./age (years)/sex	Hoehn and Yahr stage	Disease duration (years)	Autonomic dysfunction	Cerebellar dysfunction	Pyramidal sign	MRI findings	L-DOPA response
1/79/Female	III	1	+	+	+	Put	+
2/73/Female	III	1	+	+	+	Put	+
3/66/Female	I	2	+	+	+	No findings	–
4/61/Female	IV	2	+	+	+	cbll/put	–
5/72/Male	V	3	+	–	+	Put	–
6/56/Male	IV	4	+	+	+	Pons/cbll/put	–
7/73/Female	III	6	+	+	+	Pons/cbll/put	–
8/71/Female	V	9	+	–	+	Put	–

Signal change in the pons/middle cerebellar peduncles includes pontine/cerebellar atrophy (pons/cbll); Slit-like signal change at the posterolateral putaminal margin includes putaminal atrophy (put)L-DOPA, L-3,4,dihydroxyphenyl-alanine.

(MRI) examination was also performed. The characteristics of the patients are presented in Table 1. Among the eight cases of MSA-P, cases 1 and 2 apparently responded to L-DOPA at the time of the PET study, and the improvement in the symptoms of parkinsonism due to L-DOPA was confirmed by neurologists.

The healthy control group consisted of eight participants (five men and three women, 62.3±6.9 years old) that did not have a past medical history of neurological and psychiatric disorders. They were diagnosed as normal after physical and neurological examinations, screening MRI scans, and Mini-Mental Scale Evaluation (>28). They had not taken any neuroleptic drugs and were not addicted to alcohol; no history of any other substance abuse was present.

Positron emission tomography scans

^{11}C-labeled 2β-carbomethoxy-3β-(4-fluorophenyl)-tropane ([^{11}C]CFT) as a marker of presynaptic dopaminergic function for dopamine transporters and ^{11}C-labeled raclopride ([^{11}C]RAC) as a marker of postsynaptic dopaminergic function for dopamine D_2-like receptors were used as tracers for PET [7,8]. The methods used for the preparation of the radiopharmaceuticals were as described previously [9,10].

All the participants underwent the two PET studies on the same day with a 3–4-h interval. PET images were acquired in three-dimensional mode using the SET-2400W (Shimadzu, Kyoto, Japan) scanner [11] at the Positron Medical Center, Tokyo Metropolitan Institute of Gerontology. The acquired PET images were 128 × 128 × 50 in matrix size with a 2 × 2 × 3.125-mm voxel size. In PET acquisition, 300 MBq each of [^{11}C]CFT and [^{11}C]RAC were administered by an intravenous bolus injection, and all participants rested in a supine position with their eyes open during the test. The specific activity and the amount of cold material injected were 5.4–47 MBq/nM and 1.2–8.6 nM, respectively, for [^{11}C]CFT and 10–130 MBq/nM and 0.42–3.1 nM, respectively, for [^{11}C]RAC. For three of the eight healthy control participants, a dynamic scan was performed for 90 min for the [^{11}C]CFT study in the morning and for 60 min for the [^{11}C]RAC study in the afternoon to estimate the binding potentials. To measure the uptakes of these two tracers, for the five healthy participants and all the patients, a static scan was performed 75–90 min after the injection of the [^{11}C]CFT and 40–55 min after the injection of [^{11}C]RAC, respectively. The attenuation was corrected by a transmission scan using a ^{68}Ga/^{68}Ge source.

Data analysis

The two PET images of the [^{11}C]CFT and [^{11}C]RAC examinations obtained from the same participant were coregistered using an automated image registration program [12]. The images were processed further using Dr View software (AJS, Tokyo, Japan) on Linux workstations. Next, the images were resliced in the transaxial direction parallel to the anterior–posterior intercommissural (AC-PC) line, and the regions of interest (ROIs) were placed on the three subregions of the striatum – the bilateral caudate nuclei, anterior putamen, and posterior putamen – in two slices, that is, the AC-PC plane and 3.1 mm above the AC-PC line. ROIs of the striatum consisted of circles of 8-mm diameter. On each side of each slice, we set one ROI in the caudate and two ROIs each in the anterior and posterior putamen. The reference regions of the occipital lobe were placed in four slices in a range of 12.5–21.9 mm above the AC-PC plane. The reference region of the occipital lobe consisted of circles of 10-mm diameter, and we set four such circles on each side of each slice.

First, for dynamic scan data, the binding potential of the tracer in the bilateral caudate nuclei, anterior putamen, and posterior putamen of three healthy participants was estimated by a simplified reference region model [13] using the occipital lobe as a reference. Second, for static imaging, the uptake ratio index (URI) was calculated for all participants by the following formula:

$$\mathrm{URI} = (\mathrm{Activity}_{\mathrm{Striatumsubregion}} - \mathrm{Activity}_{\mathrm{Occipitallobe}})/\mathrm{Activity}_{\mathrm{Occipitallobe}}$$

URI was also calculated for the dynamic scan in the three healthy control participants using the data obtained from an equivalent time-frame. The URI in each ROI was compared between MSA-P patients and control participants with the Mann–Whitney *U*-test with Bonferroni's correction for multiple comparisons.

Next, we examined the correlation between the binding potential and the URI.

Results

For each tracer, the URIs of the striatal subregions in the static image were linearly correlated with the binding potentials in the dynamic scan (r^2=0.92, P<0.0001 for [^{11}C]CFT and r^2=0.93, P<0.0001 for [^{11}C]RAC). Therefore, we adopt the URI in reference to the occipital cortex for the further analysis.

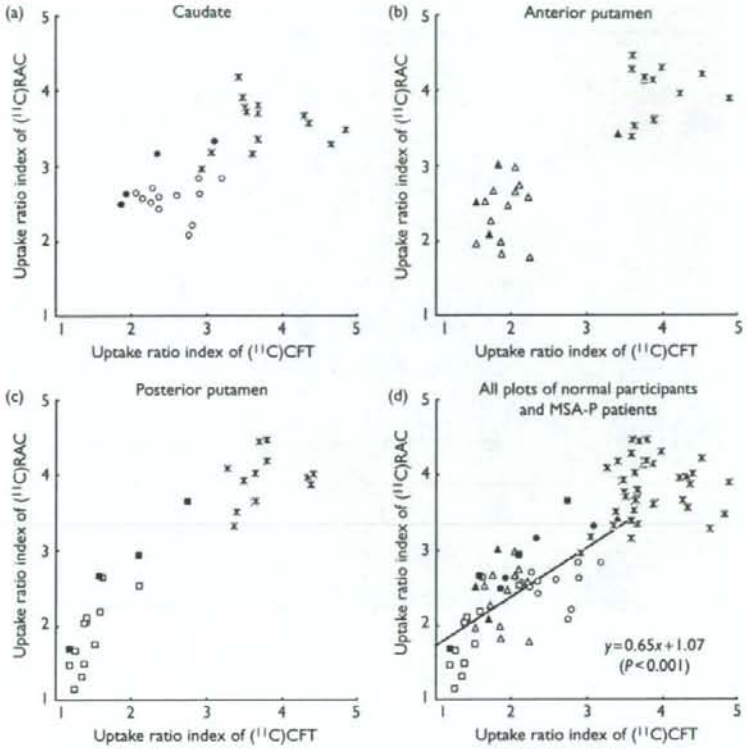

Fig. 2 The correlation between the uptake ratio index (URI) of [^{11}C]CFT and that of [^{11}C]RAC in the caudate nuclei (a), anterior putamen (b), posterior putamen (c), and all these areas (d) of all participants including MSA-P patients (n=8) and normal participants (n=8). The approximate lines for all the plots of the MSA-P group are shown in (d). Asterisk (*), normal participants; open circles (○), the caudate nuclei in MSA-P patients; open triangles (△), the anterior putamen in MSA-P patients; open squares (□), the posterior putamen in MSA-P patients; and solid markers (●), MSA-P patients exhibiting L-DOPA responsiveness. [^{11}C]CFT, ^{11}C-labeled 2β-carbomethoxy-3β-(4-fluorophenyl)-tropane; [^{11}C]RAC, ^{11}C-labeled raclopride; L-DOPA, L-3,4,dihydroxyphenyl-alanine; MSA-P, phenotype of multiple system atrophy.

Using [^{11}C]CFT and [^{11}C]RAC, we simultaneously measured presynaptic and postsynaptic nigrostriatal dopaminergic functions and observed that both functions were significantly impaired in all eight patients with MSA-P compared with the normal group.

The functional impairment in the striatum was more noticeable in the putamen, particularly in its posterior part, than in the caudate nuclei. The most prominent result of our study was that a strong positive correlation was noted between presynaptic and postsynaptic functional impairments in the MSA-P group throughout the striatum regardless of the severity of the impairments. In Parkinson's disease (PD), presynaptic and postsynaptic functional impairments were reported to be negatively correlated in the putamen by PET using [^{11}C]CFT and [^{11}C]SCH 23390 (dopamine D_1-like receptor probe), reflecting severe impairment in the presynaptic marker with an upregulation of the postsynaptic function [18]. The differential diagnosis between MSA-P and PD in clinical situations is at times difficult. The patterns of presynaptic and postsynaptic functional impairments, however, demonstrated by PET contrasted between MSA-P and PD, and therefore the two disorders can be clearly differentiated with combined presynaptic and postsynaptic dopaminergic PET examinations.

Ghaemi *et al.* [3] applied PET using [^{18}F]FDOPA and [^{11}C]RAC to MSA-P patients and discovered that both presynaptic and postsynaptic dopaminergic functions were reduced in the nigrostriatal dopaminergic system. They did not, however, provide information about whether the impairments in the presynaptic and postsynaptic dopaminergic function were correlated in each participant. Our study is the first to demonstrate a positive correlation between the presynaptic and postsynaptic dopaminergic function with respect to the local subdivisions of the striatum and the disease duration.

What is the pathological background of the strong correlation of presynaptic and postsynaptic markers measured by PET? Pathologically, neuronal loss and gliosis are the primary forms of impairment in MSA [2]. The neuronal loss tends to be severe in both SN and striatum; however, it is not always to the same extent [1], and there has been no report regarding the correlation of pathological findings such as glial cytoplasmic inclusion [19] and α-synuclein

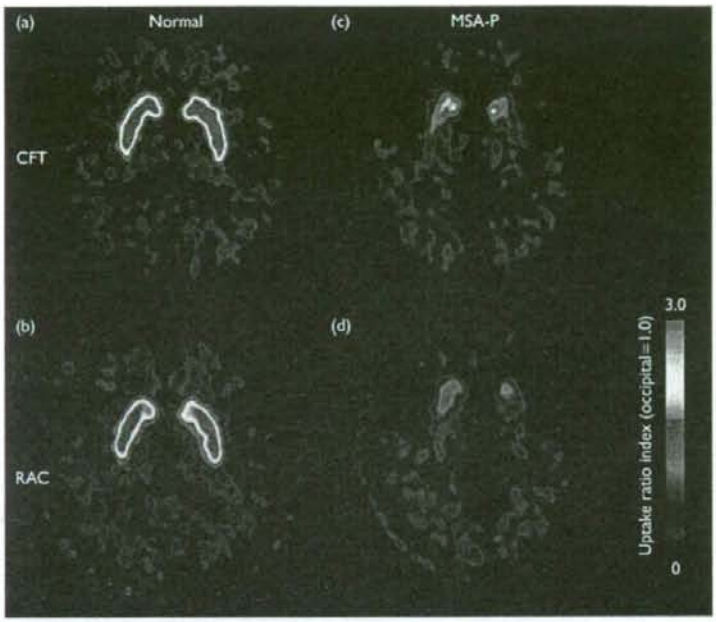

Fig. 1 Positron emission tomography images. (a) [^{11}C]CFT and (b) [^{11}C]RAC images were obtained from a normal participant, and (c) [^{11}C]CFT and (d) [^{11}C]RAC images were obtained from an MSA-P patient. All the images were normalized to the occipital lobe activity and obtained in a +3.1-mm plane from the anterior–posterior intercommissural line. [^{11}C]CFT, ^{11}C-labeled 2β-carbomethoxy-3β-(4-fluorophenyl)-tropane; [^{11}C]RAC, ^{11}C-labeled raclopride; MSA-P, phenotype of multiple system atrophy.

Table 2 The uptake ratio index of [^{11}C]CFT and [^{11}C]RAC in the subregions of the striatum

	Normal participants (n=8)	MSA-P patients (n=8)	Percentage of control
Caudate			
[^{11}C]CFT	3.70±0.55	2.49±0.41*	67.3
[^{11}C]RAC	3.46±0.40	2.63±0.31*	76.0
Anterior putamen			
[^{11}C]CFT	4.04±0.45	1.97±0.45*	48.8
[^{11}C]RAC	3.97±0.31	2.46±0.46*	62.0
Posterior putamen			
[^{11}C]CFT	3.82±0.47	1.58±0.42*	41.4
[^{11}C]RAC	3.90±0.32	2.07±0.67*	53.1

*P<0.05 as compared with normal controls (Mann–Whitney U-test with Bonferroni's multiple comparison correction).
[^{11}C]CFT, ^{11}C-labeled 2β-carbomethoxy-3β-(4-fluorophenyl)-tropane; [^{11}C]RAC, ^{11}C-labeled raclopride; MSA-P, phenotype of multiple system atrophy.

Figure 1 demonstrates the representative PET images of a normal participant and an MSA-P patient. In the MSA-P patient, the URIs of both [^{11}C]CFT and [^{11}C]RAC declined in the striatum compared with the normal participant (Fig. 1).

The results of ROI measurement are summarized in Table 2. In the MSA-P group, the URIs of both [^{11}C]CFT and [^{11}C]RAC significantly decreased in all the subdivisions of the striatum (P<0.05) in comparison with the control group, and the decrease was most prominent in the posterior putamen and relatively smaller in the caudate nuclei.

Scatter plots of the entire uptake data in individual participants for each of the three regions are shown in Fig. 2a–c and those for all areas are shown in Fig. 2d. A strong positive correlation was noted between the URIs of [^{11}C]CFT and [^{11}C]RAC in the MSA-P group. That is, the impairment of presynaptic and postsynaptic nigrostriatal dopaminergic function was observed in associative degree in all the subregions of the striatum.

Two patients apparently responded to the L-DOPA administration at the time of PET studies. Figure 2 indicates that the decrease in the [^{11}C]RAC uptake was relatively lesser in comparison with that in the [^{11}C]CFT uptake in the L-DOPA-responsive cases.

Discussion

In earlier studies, the cerebellum has been widely used as a reference region to estimate the availability of dopamine transporters using [^{11}C]CFT [14,15] and dopamine D_2-like receptors using [^{11}C]RAC [16]. We, however, selected the occipital cortex as a reference region in this study. Neuropharmacological evidence has revealed that the densities of both the dopamine transporters and dopamine D_2-like receptors in the human occipital cortex are negligible as in the case of the cerebellum [17]. Furthermore, the cerebellum is often involved in the pathological processes in MSA-P, whereas the occipital lobe is less likely to be affected. The selection of the occipital region as a reference would be useful for PET analysis of MSA. In contrast, the measured values of the striatum might have affected by the atrophy. The correlation of two PET measures on the same regions, however, are robust because they are evaluated with common ROIs to cancel out the spatial effect.

[20,21] between SN and striatum. If the PET markers for presynaptic and postsynaptic dopaminergic function directly reflect the degree of degeneration in SN and striatum independently, as in PD [15,22], the combination in the degree of presynaptic and postsynaptic functional impairment could be variable. The presence of a strong positive correlation between the presynaptic and postsynaptic dopaminergic functions measured by PET within participants and across participants suggests that these impairments in MSA-P are the result of the destruction of the entire synaptic structure in the striatum. Pathologically, the putamen is one of the areas with the most severe neuronal loss in MSA-P [2]. We consider that the presynaptic marker represents the degree of degeneration of the SN only if the striatum involvement is lesser than that of SN; however, once the severe destruction of striatum occurs, the presynaptic marker no longer represents the degree of SN degeneration because it is masked by the destruction of the entire structure of the synapse.

Parkinsonism in MSA is treated with L-DOPA, dopamine agonists, and anticholinergic agents; however, only a mild effect is noted in a minor population in the early stage, and the responsiveness to L-DOPA gradually disappears. Generally, responses to L-DOPA are poor in cases of MSA-P [1]. In a previous report, L-DOPA was effective in the early stage in approximately 1/3 of the MSA cases [23]. We examined two early MSA-P cases responsive to L-DOPA. In these cases, the presynaptic dopaminergic function was markedly reduced; however, the reduction in the postsynaptic dopaminergic function was relatively less severe compared with that in the cases not responsive to L-DOPA; moreover, this trend was more prominent in the striatum on the contralateral side in which L-DOPA alleviated the symptoms of parkinsonism. Churchyard *et al.* [24] suggested that the ineffectiveness of L-DOPA on parkinsonism in MSA is related to the dominance of neuronal loss, gliosis, and the reduction in postsynaptic dopamine D_2 receptors in the posterior putamen. Wenning *et al.* [5] reported that L-DOPA was highly effective in the cases in which the putamen was relatively conserved compared with the degree of nigral neuronal loss, and the effect of L-DOPA was negatively correlated with the degree of nigral degeneration, suggesting that nigral degeneration precedes striatal degeneration [1]. Whether nigral degeneration preceded striatal degeneration was not clear in our study; however, postsynaptic dopaminergic function was relatively retained in our L-DOPA-responsive cases. We consider that the degree of conservation of postsynaptic dopaminergic function is related to the effectiveness of L-DOPA in MSA-P and that a trend of dissociation of presynaptic and postsynaptic markers can be detected by PET. Further studies are necessary to increase the number of the participants and to follow up the L-DOPA-responsive cases using PET and clinical course observations.

Conclusion

We have established the presence of a strong positive correlation between the reductions in nigrostriatal presynaptic and postsynaptic dopaminergic functions and L-DOPA-responsive cases in which the degrees of presynaptic and postsynaptic functional impairments are dissociated in some manner.

The elucidation of the patterns and processes of presynaptic and postsynaptic functional impairments may provide a clue to understanding the development and advancement mechanisms of the disease and will aid in a more reliable early clinical diagnosis and prediction of drug effects.

References

1. Wenning GK, Ben-Shlomo Y, Magalhaes M, Daniel SE, Quinn NP. Clinicopathological study of 35 cases of multiple system atrophy. *J Neurol Neurosurg Psychiatry* 1995; 58:160–166.
2. James SL, Nigel L. Disorders of movement and system degeneration. In: David IG, Peter LL, editors. *Greenfield's neuropathology*. 7th ed. Vol. 2. London: Arnold; 2002. pp. 325–430.
3. Ghaemi M, Hilker R, Rudolf J, Sobesky J, Heiss WD. Differentiating multiple system atrophy from Parkinson's disease: contribution of striatal and midbrain MRI volumetry and multi-tracer PET imaging. *J Neurol Neurosurg Psychiatry* 2002; 73:517–523.
4. Van Royen E, Verhoeff NP, Speelman JD, Wolters EC, Kuiper MA, Janssen AG. Multiple system atrophy and progressive supranuclear palsy. Diminished striatal D_2 dopamine receptor activity demonstrated by ^{123}I-IBZM single photon emission computed tomography. *Arch Neurol* 1993; 50:513–516.
5. Wenning GK, Quinn N, Magalhaes M, Mathias C, Daniel SE. 'Minimal change' multiple system atrophy. *Mov Disord* 1994; 9:161–166.
6. Gilman S, Low P, Quinn N, Albanese A, Ben-Shlomo Y, Fowler C, *et al.* Consensus statement on the diagnosis of multiple system atrophy. American Autonomic Society and American Academy of Neurology. *Clin Auton Res* 1998; 8:359–362.
7. Volkow ND, Fowler JS, Gatley SJ, Logan J, Wang GJ, Ding YS, *et al.* PET evaluation of the dopamine system of human brain. *J Nucl Med* 1996; 37:1242–1256.
8. Booij J, Tissingh G, Winogrodzka A, van Royen EA. Imaging of the dopaminergic neurotransmission system using single-photon emission tomography and positron emission tomography in patients with parkinsonism. *Eur J Nucl Med* 1999; 26:171–182.
9. Kawamura K, Oda K, Ishiwata K. Age-related changes of the [^{11}C]CFT binding to the striatal dopamine transporters in the Fischer 344 rats: a PET study. *Ann Nucl Med* 2003; 17:249–253.
10. Langer O, Någren K, Dolle F, Lundkvist C, Sandell J, Swahn CG, *et al.* Precursor synthesis and radiolabelling of the dopamine D_2 receptor ligand [^{11}C]raclopride from [^{11}C]methyl triflate. *J Labelled Comp Radiopharm* 1999; 42:1183–1193.
11. Fujiwara T, Watanuki S, Yamamoto S, Miyake M, Seo S, Itoh M, *et al.* Performance evaluation of a large axial field-of-view PET scanner : SET-2400W. *Ann Nucl Med* 1997; 11:307–313.
12. Ardekani BA, Braun M, Hutton BF, Kanno I, Iida H. A fully automatic multimodality image registration algorithm. *J Comput Assist Tomogr* 1995; 19:615–623.
13. Gunn RN, Lammertsma AA, Hume SP, Cunningham VJ. Parametric imaging of ligand-receptor binding in PET using a simplified reference region model. *NeuroImage* 1997; 6:279–287.
14. Wong DF, Yung B, Dannals RF, Shaya EK, Ravert HT, Chen CA, *et al.* In vivo imaging of baboon and human dopamine transporters by positron emission tomography using [^{11}C]WIN 35 428. *Synapse* 1993; 15:130–142.
15. Frost JJ, Rosier AJ, Reich SG, Smith JS, Ehlers MD, Snyder SH, *et al.* Positron emission tomographic imaging of the dopamine transporter with ^{11}C-WIN 35,428 reveals marked declines in mild Parkinson's disease. *Ann Neurol* 1993; 34:423–431.
16. Antonini A, Leenders KL, Reist H, Thomann R, Beer HF, Locher J. Effect of age on D_2 dopamine receptors in normal human brain measured by positron emission tomography and ^{11}C-raclopride. *Arch Neurol* 1993; 50:474–480.
17. Mozley PD, Stubbs JB, Kung HF, Selikson MH, Stabin MG, Alavi A. Biodistribution and dosimetry of iodine-123-IBF: a potent radioligand for imaging the D2 dopamine receptor. *J Nucl Med* 1993; 34:1910–1917.
18. Ouchi Y, Kanno T, Okada H, Yoshikawa E, Futatsubashi M, Nobezawa S, *et al.* Presynaptic and postsynaptic dopaminergic binding densities in the nigrostriatal and mesocortical systems in early Parkinson's disease: a double-tracer positron emission tomography study. *Ann Neurol* 1999; 46:723–731.

19. Papp MI, Kahn JE, Lantos PL. Glial cytoplasmic inclusions in the CNS of patients with multiple system atrophy (striatonigral degeneration, olivopontocerebellar atrophy and Shy–Drager syndrome). *J Neurol Sci* 1989; **94**:79–100.
20. Tu PH, Galvin JE, Baba M, Giasson B, Tomita T, Leight S, *et al*. Glial cytoplasmic inclusions in white matter oligodendrocytes of multiple system atrophy brains contain insoluble alpha-synuclein. *Ann Neurol* 1998; **44**:415–422.
21. Wakabayashi K, Yoshimoto M, Tsuji S, Takahashi H. Alpha-synuclein immunoreactivity in glial cytoplasmic inclusions in multiple system atrophy. *Neurosci Lett* 1998; **249**:180–182.
22. Snow BJ, Tooyama I, McGeer EG, Yamada T, Calne DB, Takahashi H, *et al*. Human positron emission tomographic [^{18}F]fluorodopa studies correlate with dopamine cell counts and levels. *Ann Neurol* 1993; **34**:324–330.
23. Rajput AH, Rozdilsky B, Rajput A, Ang L. Levodopa efficacy and pathological basis of Parkinson syndrome. *Clin Neuropharmacol* 1990; **13**:553–558.
24. Churchyard A, Donnan GA, Hughes A, Howells DW, Woodhouse D, Wong JY, *et al*. Dopa resistance in multiple-system atrophy: loss of postsynaptic D_2 receptors. *Ann Neurol* 1993; **34**:219–226.

J Neuropathol Exp Neurol
Copyright © 2008 by the American Association of Neuropathologists, Inc.

Vol. 67, No. 10
October 2008
pp. 945–953

ORIGINAL ARTICLE

Lewy Body Pathology Involves Cutaneous Nerves

Masako Ikemura, MD, PhD, Yuko Saito, MD, PhD, Renpei Sengoku, MD, Yoshio Sakiyama, MD, PhD, Hiroyuki Hatsuta, MD, Kazutomi Kanemaru, MD, PhD, Motoji Sawabe, MD, PhD, Tomio Arai, MD, PhD, Genta Ito, MS, Takeshi Iwatsubo, MD, PhD, Masashi Fukayama, MD, PhD, and Shigeo Murayama, MD, PhD

Abstract

Involvement of the peripheral autonomic nervous system is a core feature of Lewy body (LB) diseases, including Parkinson disease (PD), PD with dementia, and dementia with LBs. To investigate the potential use of skin biopsy for the diagnosis of LB diseases, we assessed anti-phosphorylated α-synuclein immunoreactivity in peripheral nerves in samples of skin from the abdominal wall and flexor surface of the upper arm in 279 prospectively studied consecutively autopsied patients whose data were registered at the Brain Bank for Aging Research between 2002 and 2005. Positive immunoreactivity was demonstrated in the unmyelinated fibers of the dermis in 20 of 85 patients with LB pathology in the CNS and the adrenal glands, the latter representing a substitute for peripheral autonomic nervous system sympathetic ganglia; no reactivity was seen in 194 patients without CNS LB pathology. In 142 retrospectively studied patients autopsied from 1995 onward who had subclinical or clinical LB disease, the sensitivity of the positive skin immunoreactivity was 70% in PD and PD with dementia and 40% in dementia with LBs. Skin immunoreactivity was absent in cases of multiple-system atrophy, progressive nuclear palsy, and corticobasal degeneration. We demonstrate for the first time that the skin is involved and may be a highly specific and useful biopsy site for the pathological diagnosis of LB diseases.

Key Words: α-Synuclein Adrenal gland, Dementia with Lewy bodies, Dermis, Immunohistochemistry, Lewy bodies, Parkinson disease.

INTRODUCTION

Lewy body (LB) diseases (LBDs) (1) are defined by neuronal degeneration related to the presence of LBs; they include Parkinson disease, either with normal cognition (PD) or with dementia (PDD), dementia with LBs (DLB), and LB-related progressive autonomic failure (LBPAF) (2). Involvement of the peripheral autonomic nervous system (PANS) is a key feature of LBD and is a presenting clinical feature in some cases of PD, PDD, DLB, and LBPAF. Autonomic dysfunction can greatly influence the patient's prognosis and quality of life.

Pathological studies of the PANS demonstrate LB pathology involving the sympathetic and enteric nervous systems (3–8). Recently, ^{123}I-metaiodobenzylguanidine cardiac scintigraphy has become widely accepted in Japan as a tool for the diagnosis of LBD (9, 10); the pathological basis of this test is the presence of LB pathology of the sympathetic nerve fibers that supply epicardial fatty tissue (11).

There is a general consensus among neuropathologists that the standard organ for pathological evaluation of the PANS in LBD is the sympathetic ganglion (12), but autopsy sampling of the sympathetic ganglia can be difficult. We recently reported that the adrenal gland—one of the organs routinely examined at general autopsy—can be used as a substitute for the PANS sympathetic ganglia because it has similar pathological findings in LBDs (2).

The anatomical structures identified to date as having LB pathology are not appropriate biopsy sites for the premortem diagnosis of LBDs. In 2002, we examined skin excised near a decubitus ulcer at autopsy from a patient with DLB and found positive immunoreactivity with anti-phosphorylated α-synuclein antibodies in an unmyelinated fiber in the dermis. This observation prompted us to examine skin sampled from consecutively autopsied patients whose data were registered in the Brain Bank for Aging Research (BBAR).

From the Department of Neuropathology, Tokyo Metropolitan Institute of Gerontology (MI, YuS, RS, YoS, HH, SM); Department of Human Pathology (MI, MF), Graduate School of Medicine, The University of Tokyo; Department of Pathology, Tokyo Metropolitan Geriatric Hospital (YuS, MS, TA); Department of Neurology, The Jikei University School of Medicine (RS); Department of Neurology, Tokyo Metropolitan Geriatric Hospital (KK); and Department of Neuropathology and Neuroscience, Graduate School of Medicine, The University of Tokyo (GI, TI), Tokyo, Japan.

Send correspondence and reprint requests to: Yuko Saito, MD, PhD, Department of Pathology, Tokyo Metropolitan Geriatric Hospital, 35-2 Sakaecho, Itabashi-ku, Tokyo 173-0015; E-mail: yukosa@tmig.or.jp

Masako Ikemura is now with the Department of Pathology, Teikyo University School of Medicine, Tokyo, Japan.

Grants-in-aid: Aid for Scientific Research on Priority Areas—Advanced Brain Science Project (SM, YuS) and Aid for Basic Scientific Research B (SM) and C (YuS) from the Ministry of Education, Culture, Sports, Science, and Technology of Japan; Aid for Degenerative Disease (SM), Neurological and Psychiatric Research (SM, YuS) and Research for Longevity (SM, YuS) from the Ministry of Health, Labor, and Welfare of Japan; Aid for Long-Term Comprehensive Research on Age-Associated Dementia from the Tokyo Metropolitan Institute of Gerontology (SM); Grant from The Novartis Foundation for Gerontological Research (2006) (YuS), Grant from the Tokyo Metropolitan Geriatric Hospital (YuS).

Copyright © 2008 by the American Association of Neuropathologists, Inc. Unauthorized reproduction of this article is prohibited.

MATERIALS AND METHODS

Tissue Sources

The study consisted of 2 parts. The first part was a prospective study to determine the specificity of LBD in the skin in relation to LBD in the CNS and PANS. The second part was a retrospective study to determine the sensitivity of detection of LBD in the skin in relation to LBD in the CNS and PANS. The data registered in BBAR were from consecutively autopsied patients from a general geriatric hospital; informed consent was obtained from the relatives at autopsy (2, 13, 14).

In the prospective study, we used routinely sampled abdominal skin and prospectively sampled brachial skin from 279 consecutive autopsy patients whose data were registered in BBAR between 2002 and 2005. The patients' ages ranged from 52 to 104 years (mean, 80.8 ± 8.6 [SD] years); the male-to-female ratio was 167:112. The postmortem interval ranged from 52 minutes to 88 hours (mean, 13 hours). This series included 8 patients with progressive supranuclear palsy and 3 patients with corticobasal degeneration.

A wedge-shaped brachial skin sample, 1 cm × 0.5 cm in area and including the dermis and subcutaneous fatty tissue, was directly fixed in 4% paraformaldehyde for 48 hours and then embedded in paraffin. The abdominal skin had been routinely sampled since 1995, fixed in 10% buffered formalin for at least a week, and then embedded in paraffin. We used fixation in 4% paraformaldehyde for 48 hours because this fixation increased sensitivity for Lewy neurite detection in the CNS. We also continued to fix abdominal skin in 10% buffered formalin because the fixation is generally accepted and more applicable to potential biopsy in the clinic.

In the retrospective study, from among 1,594 patients whose data had been consecutively registered in BBAR between 1995 and 2005, we used 142 cases with the postmortem diagnosis of CNS LB stage II or greater (see later). The results of abdominal skin samples from 33 patients, who had been registered from 2002 onward and were also used in the prospective study, were included in the retrospective study to increase the case number for statistical analysis. Archival paraffin blocks of abdominal skin from the additional 109 patients from the period between 1995 and 2001 were stained as in the prospective study. The age range of the 142 patients was from 48 to 100 years (mean, 83.7 ± 7.6 years); the male-to-female ratio was 72:70. Abdominal skin samples from 3 cases with multiple-system atrophy (MSA; 1 case of MSA-P and 2 cases of MSA-C) from this period were also examined for comparison because no patient of MSA was included in the prospective studies. This study was approved by the institutional review boards of the Tokyo Metropolitan Institute of Gerontology and the Tokyo Metropolitan Geriatric Hospital.

Clinical Information

Clinical data, including information on the presence or absence of parkinsonism and cognitive state, were obtained from medical charts, as previously reported (13, 14). Final locomotive activity was classified into 4 levels: bedridden, wheelchair-bound, cane-assisted, and independent walking. In addition, the presence of decubitus ulcers was noted from the prosecutors' records at autopsy.

Pathological Examination of the Skin

Six-micrometer-thick serial paraffin sections of the skin were stained with hematoxylin and eosin and by immunohistochemistry with an autoimmunostainer (20NX; Ventana, Tucson, AZ) for single or double immunolabeling, as previously reported (15). All antibodies used are listed in Table 1.

For LB pathology, the antibodies used were anti-phosphorylated α-synuclein (psyn) (psyn no. 64 [16] monoclonal and PSer129 [17] polyclonal). One section each of 2 serial sections was used for the staining of monoclonal and polyclonal anti-psyn antibodies. In addition, selected sections were double-immunostained with psyn and anti-phosphorylated neurofilament monoclonal antibody (SMI31).

TABLE 1. Antibodies

Antibody	Clone	Epitope	Source	Animal	Dilution Ratio	Antigen Retrieval
psyn no. 64	Monoclonal	α-Synuclein phosphorylated ser129	T. Iwatsubo (available from Wako, Tokyo, Japan)	Mouse	1:20000 for CNS	Formic acid
					1:10000 for skin	Formic acid
PSer129	Polyclonal	α-Synuclein phosphorylated ser129	T. Iwatsubo	Rabbit	100	none
Ubiquitin	Polyclonal	Ubiquitin	DAKO, Glostrup, Denmark	Rabbit	1:1000	Microwave in citrate buffer
AT8	Monoclonal	τ-Phosphorylated Ser-202 and Thr-205	Innogenetics, Temse, Belgium	Mouse	1:1000	None
12B2	Monoclonal	Aβ11–28 a.a.	IBL, Maebashi, Japan	Mouse	1:50	Formic acid
GFAP	Polyclonal	Glial fibrillary acidic protein	DAKO	Rabbit	1:10	None
CD68	Monoclonal	CD68	DAKO	Mouse	1:100	Microwave in citrate buffer
TH	Monoclonal	Tyrosine hydroxylase	Calbiochem-Novabiochem, Darmstadt, Germany	Mouse	1:10000	Microwave in target retrieval solution (DAKO)
SMI31	Monoclonal	Phosphorylated neurofilament	Sternberger Immunochemicals, Bethesda, MD	Mouse	1:20000	None

GFAP, glial fibrillary acidic protein; TH, tyrosine hydroxylase.

© 2008 American Association of Neuropathologists, Inc.

Copyright © 2008 by the American Association of Neuropathologists, Inc. Unauthorized reproduction of this article is prohibited.

Double labeling immunofluorescence studies were performed by incubating sections with anti-psyn antibody (PSer129, polyclonal) and anti-tyrosine hydroxylase (TH) antibody; for labeling, anti-rabbit Alexa 546 Fluor (Molecular Probes, Eugene, OR) (red) and immunoglobulin G Alexa 488 (green) were used. Sections were viewed under a Zeiss confocal laser scanning microscope (model LSM5 PASCAL; Jena, Germany).

For immunoelectron microscopy, we used selected paraffin sections stained with PSer129 and visualized using diaminobenzidine. The sections were evaluated by light microscopy and washed in a 0.1% (pH 7.4) phosphate buffer, postfixed in 1% osmium tetroxide, dehydrated in a graded series of ethanol, and embedded in epoxy resin. Plastic capsules filled with fresh epoxy resin were placed on the appropriate area of the sections and after polymerization of the resin, the target tissues were stripped off from the glass slides to the top of the epoxy resin. Ultrathin sections were then obtained and were examined under an H-7500 electron microscope (Hitachi, Japan) without a counterstain.

The BBAR Protocols for Evaluating Pathology of the CNS

The brains and spinal cords from all the patients of both the retrospective and the prospective studies were examined as previously reported (14). Briefly, 6-μm-thick sections were stained with hematoxylin and eosin and by the Klüver-Barrera method; selected sections were further examined with modified methenamine and Gallyas-Braak silver staining for senile changes, Congo red for amyloid deposition, and elastica Masson trichrome stain for vascular changes. In addition, selected sections were stained using the anti-α-synuclein and anti-ubiquitin antibodies (Table 1). To evaluate other senile changes, antibodies against phosphorylated tau, amyloid β (Aβ), glial fibrillary acidic protein, CD68, and phosphorylated neurofilament were also used.

Lewy body-related pathology in the CNS was examined at several levels of the thoracic spinal cord and in the medulla oblongata at the level of the dorsal motor nucleus of the vagus, the upper pons at the level of the locus ceruleus, the midbrain, the cerebellum (including the dentate nucleus), the basal ganglia (including the basal nucleus of Meynert), the amygdala, and the posterior hippocampus. In addition, areas were evaluated for LB scores according to the first and revised consensus guidelines for DLB (18, 19). These areas included the anterior cingulate gyrus, the entorhinal cortex, the second frontal and temporal gyri, and the supramarginal gyrus. Samples from these areas were stained by immunohistochemistry and classified into 7 CNS LB stages according to previously reported criteria (2, 14, 16) as follows: LB stage 0, no LBs; LB stage 0.5, Lewy neurites alone or diffuse or fine granular cytoplasmic staining lacking any focal aggregates in sections stained with anti-psyn antibodies; LB stage I, scattered LBs without cell loss (incidental LBD); LB stage II, abundant LBs with macroscopic loss of pigmentation in substantia nigra and locus ceruleus and/or gliosis demonstrated by glial fibrillary acidic protein immunohistochemistry in areas containing LBs but without attributable parkinsonism or dementia (subclinical LBD); LB stage III, PD without dementia; LB stage IV, DLB or PDD, transitional (limbic) form (DLBT or PDDT); and LB stage V, DLB or PDD, neocortical form (DLBN or PDDN). Parkinson disease with dementia was differentiated from DLB based on the definition in the consensus guidelines that "[PDD] dementia appears more than 12 months after the onset of parkinsonism." The CNS LB stages are shown in Table 2. We subcategorized CNS stages I and II into primary and secondary α-synucleinopathy on the basis of our previous work (14, 16). Primary α-synucleinopathy involved the intermediolateral column of the spinal cord or the preganglionic sympathetic neurons and was further subdivided into brainstem, transitional, and neocortical forms according to the LB score or distribution. Secondary α-synucleinopathy spared the

TABLE 2. Lewy Body Stages in the CNS

Stage	Substantia Nigra and Locus Ceruleus: Loss of Pigmentation	LB					Dementia	PA	Diagnosis
		Nigrostriatal	Limbic-neocortical	Spinal Cord	LB Score	Adrenal (2)			
0	−	−	−	−	0	+/−			
0.5	−	+/−	+/−	+/−	0	+/−			
I	−	+/−	+/−	+/−	0	+/−			Incidental LBD
II	+	+	+/−	+/−	0–10	+/−	−*	−*	Subclinical LBD
III	+	+	+	+	0–10	+	−	+	PD
IV P	+	+	+	+	3–6	+	+	+	PDDT
IV D	+	+	+	+	3–6	+/−	+	+/−	DLBT†
V P	+	+	+	+	7–10	+	+	+	PDDN
V D	+	+	+	+	7–10	+/−	+	+/−	DLBN†

*No dementia or parkinsonism associated with LB-related α-synucleinopathy.

†Differential diagnosis of PDD and DLB was based on the "1-year rule" in the consensus guidelines (19).

All patients with PD or PDD had adrenal LBD (2).

DLBN, dementia with LBs, with an LB score corresponding to the value for the neocortical form; DLBT, dementia with LBs, with an LB score corresponding to the value for the transitional form; LB, Lewy body; LBD, LB disease; PA, parkinsonism; PD, Parkinson disease; PDDN, PD with dementia, with an LB score corresponding to the value for the neocortical form; PDDT, PD with dementia, with an LB score corresponding to the value for the transitional form.

© 2008 American Association of Neuropathologists, Inc.

Copyright © 2008 by the American Association of Neuropathologists, Inc. Unauthorized reproduction of this article is prohibited.

preganglionic sympathetic neurons, preferentially involved the amygdala, and was termed *amygdala variant*.

Evaluation of Pathology Related to Other Senile Changes

Neurofibrillary tangles were classified into 7 stages and senile plaques into 4 stages according to Braak criteria (20). Argyrophilic grains were classified into the 4 stages that we previously reported (13). National Institute on Aging-Reagan criteria modified by us were adopted for the diagnosis of Alzheimer disease (AD) (21). Diagnoses of "dementia with grains" and "neurofibrillary-tangle-predominant form of dementia" were based on Jellinger's definitions (22, 23).

Pathological Study of the PANS

The adrenal glands were evaluated in the 279 patients in the prospective study, as previously reported (2). The adrenal glands from the additional 109 patients in the retrospective study were also examined for adrenal LB pathology. Data on 47 of these 109 patients were included in our previous report (2).

Statistical Analysis

Statistical analysis was performed by the χ^2 test for comparisons of categorical data. Statistical significance was established at $p < 0.05$.

RESULTS

Prospective Study

LB Pathology in the Skin

Immunohistochemical staining with anti-psyn antibodies demonstrated positive neurites and dots in nerve fascicles of the dermis and subcutaneous tissue (Figs. 1A, B). In some cases, psyn-positive nerve fibers showed swellings (Figs. 1C, D). Psyn-positive small dots or thin linear structures were also found around blood vessels (Figs. 1E, F). These psyn-positive structures seemed to colocalize with the

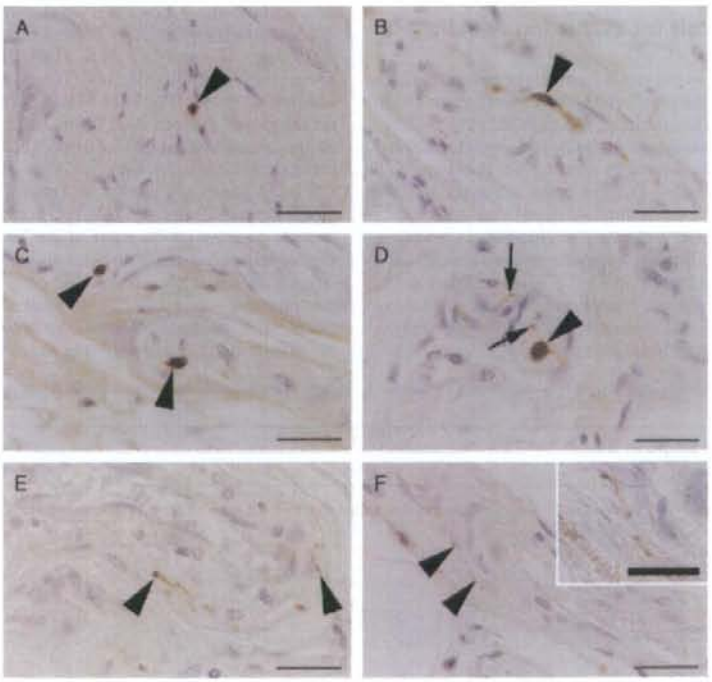

FIGURE 1. Immunohistochemical staining of nerve fascicles and vascular walls in the skin with anti-phosphorylated α-synuclein (psyn) antibodies. **(A)** Dotlike immunoreactivity (arrowhead) in a cross section of a nerve fascicle. **(B)** Longitudinal section of a cutaneous nerve with threadlike psyn immunoreactivity with a focal swelling (arrowhead). **(C)** Oval areas of immunoreactivity (arrowheads) scattered in nerve fascicles. **(D)** An oval structure connected to a linear structure (arrowhead) and small dotlike and linear staining (arrow). **(E)** Polyclonal anti-psyn antibody reveals a thin linear structure (arrowheads), extending from a nerve fascicle to the wall of blood vessel. **(F)** Monoclonal anti-phosphorylated α-synuclein antibody detects several positive thin linear structures in a vessel wall (arrowheads). Inset shows a higher power. **(A–E)**: PSer129, polyclonal; and **(F)**: psyn no. 64, monoclonal. Scale bars = **(A–F)** 25 μm; (inset in **F)** 10 μm.

© 2008 American Association of Neuropathologists, Inc.

Copyright © 2008 by the American Association of Neuropathologists, Inc. Unauthorized reproduction of this article is prohibited.

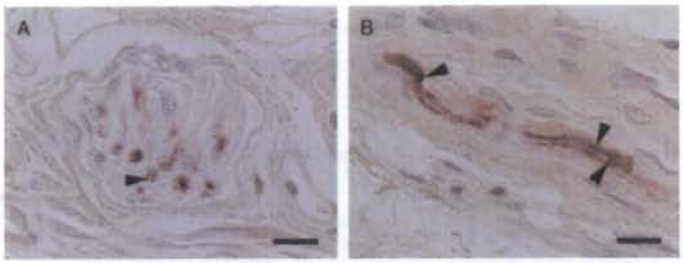

FIGURE 2. Double immunocytochemical staining with anti-phosphorylated α-synuclein (brown) and anti-phosphorylated neurofilament (red) antibodies. **(A)** In a cross section, PSer129 immunoreactivity is localized within SMI31-immunoreactive axons (arrowhead). **(B)** In a longitudinal section of a nerve fascicle, PSer 129 immunoreactivity is continuous with SMI31-immunoreactive axons (arrowheads). Scale bars = (**A, B**) 10 μm.

axons. This was confirmed by double label immunohistochemistry using antibodies to psyn and phosphorylated neurofilament (Figs. 2A, B). By confocal microscopy, psyn immunoreactivity was also colocalized with the epitope of anti-TH antibody (Fig. 3).

By electron microscopy of immunostained sections, psyn-immunoreactive structures seemed to be composed of granulofilamentous profiles among mitochondria and vesicles. The psyn-immunoreactive structures had thin filaments at their peripheries that were consistent with the size of intermediate filaments and were surrounded by basal lamina. These features are consistent with those of unmyelinated axons (Fig. 4).

Comparison of CNS LB Stages

Psyn-positive structures in the skin were very small and not always found in the 2 serial sections stained either with psyn no. 64 and PSer129. Therefore, when positive immunoreactivity was found in any of the 2 stained sections for each anatomical location, the case was counted as positive. Correlations between CNS LB stage in the prospective study and the presence or absence of α-synuclein immunoreactivity in the skin are summarized in Table 3. Psyn immunoreactivity in abdominal and brachial skin did not always match in a single patient (Table 3), but the overall frequencies were similar and were apparently unaffected by differences in the method of fixation or in anatomical location.

The numbers of patients and rates of skin positivity (%) at each stage were as follows: stage 0, none of 194 patients (0%); stage 0.5, 1 (4.0%) of 25 patients; stage I, 1 (3.7%) of 27 patients; stage II, 3 (33.3%) of 9 patients; stage III, 2 (100%) of 2 patients; stage IV, 6 (54.5%) of 11 patients; and stage V, 7 (63.6%) of 11 patients. Because all CNS LB stage 0 patients, including 8 progressive supranuclear palsy and 3 corticobasal degeneration cases, were negative for psyn immunoreactivity in the skin, there were no false-positive results, and the specificity was 100%. Among the 20 patients with psyn-positive immunoreactivity in the skin, 11 had positive immunoreactivity in both skin locations, 6 in the abdominal skin alone, and 3 in the skin of the arm alone.

Comparison With Adrenal Gland Positivity

All the patients with positive psyn immunoreactivity in the skin also had α-synucleinopathy in the adrenal glands (Table 3).

Retrospective Study

Pathology of LB-Related α-Synucleinopathy in the Skin

The numbers of patients and the rates of skin positivity (percentage) at each CNS LB stage of II or more were as follows: stage II, 13 (23.2%) of 56 patients; stage III, 10 (71.4%) of 14 patients; stage IV, 17 (44.7%) of 38 patients; stage V, 18 (52.9%) of 34 patients (Table 4). Samples from all 3 of the patients with MSA were negative.

We next examined the percentages of patients with positive psyn immunoreactivity in the skin from the abdomen in each subgroup of CNS LB stage II or subclinical LBD (Table 4). The sensitivity was approximately 20%, but was 0% for the amygdala variant cases. We then classified stage IV and V cases into PDD and DLB and compared the

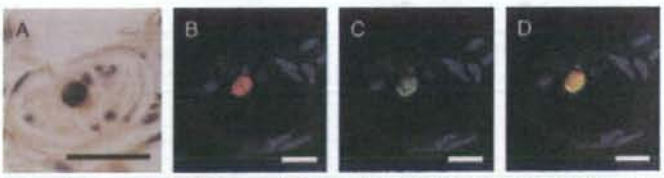

FIGURE 3. Immunohistochemical and confocal immunofluorescent localization of phosphorylated α-synuclein (PSer129) and tyrosine hydroxylase (TH). **(A)** An oval area of immunoreactivity to PSer129 in the dermal nerve. Scale bars = 25 μm. **(B–D)** Confocal images of dermal nerve showing colocalization. **(B)** Alexa 546 (red) for phosphorylated α-synuclein. **(C)** Alexa 488 (green) for TH. **(D)** View of merged (**B** and **C**). Scale bars = (**B–D**) 10 μm.

© 2008 American Association of Neuropathologists, Inc.

Copyright © 2008 by the American Association of Neuropathologists, Inc. Unauthorized reproduction of this article is prohibited.

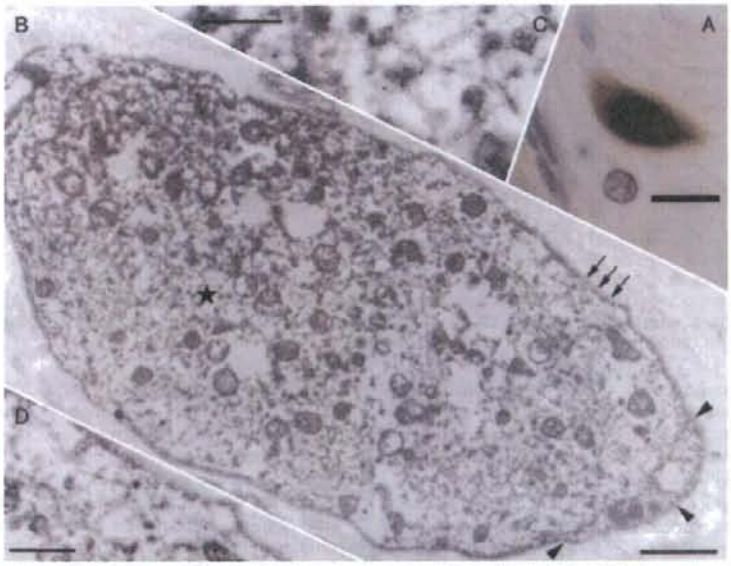

FIGURE 4. Immunoelectron microscopy of anti-phosphorylated α-synuclein antibody (PSer129)–immunoreactive structures in a dermal nerve fascicle. **(A)** Light microscopy of an immunoreactive oval profile visualized with diaminobenzidine. Scale bars = 25 μm. **(B)** Immunoelectron microscopy showing the structure shown in **(A)** surrounded by basal lamina (triple arrows) and with abundant organelles. This probably represents the cytoplasm of an unmyelinated Schwann cell (arrowheads). Scale bars = 1 μm. **(C)** High-magnification view of the area indicated by the asterisk in **(B)**, demonstrating granulofilamentous profiles among mitochondria and vesicular structures. Scale bars = 250 nm. **(D)** High-magnification view of the area indicated by the arrows in **(B)** showing thin filaments. Scale bars = 500 nm.

positivity ratios. The number of patients and positivity ratio (%) in each group were as follows: PDDT, 8 (61.5%) of 13 patients; DLBT, 9 (36%) of 25 patients; PDDN, 6 (85.7%) of 7 patients; and DLBN, 12 (44.4%) of 27 patients. Therefore, the sensitivity of LB pathology in the skin was 14 (70%) of 20 in PDD and 21 (40.4%) of 52 in DLB.

Association of Coexistent Pathology of AD or Argyrophilic Grain Disease With LB-Related Skin Pathology in PDD or DLB

Patients with PDD or DLB were classified into 2 groups: those having or not having LB-related pathology in the skin. These 2 groups were evaluated for the grade of coexistent AD

TABLE 3. Lewy Body Pathology in the Skin of the 279 Consecutive Patients Used in the Prospective Study

		LB Pathology in the Skin				Adrenal LBD
CNS LB Stage	n	Arm +/Abdomen +	Arm +/Abdomen −	Arm −/Abdomen +	Positive, %	Positive, %
0	194	0	0	0	0	1 (0.5)
0.5	25	0	0	1	1 (4.0)	1 (4.0)
I	27	0	0	1	1 (3.7)	2 (7.4)
II	9	1	1	1	3 (33.3)	6 (66.7)
III	2	2	0	0	2 (100)	2 (100)
IV	11	4	1	1	6 (54.5)	11 (100)
P	4	1	0	0	1	4 (100)
D	7	3	1	1	5	7 (100)
V	11	4	1	2	7 (63.6)	10 (90.9)
P	1	0	1	0	1	1 (100)
D	10	4	0	2	6	9 (90)
Total	279	11	3	6	20	33

Because no LB pathology was detected in the skin in cases without CNS LB pathology, the specificity of dermal LB pathology with respect to the CNS was 100%.
Abdomen, abdominal wall; Arm, flexor surface of the upper arm; D, dementia with LBs; LB, Lewy body; LBD, Lewy body disease; P, Parkinson disease with dementia.

© 2008 American Association of Neuropathologists, Inc.

Copyright © 2008 by the American Association of Neuropathologists, Inc. Unauthorized reproduction of this article is prohibited.

or argyrophilic grain disease (AGD) pathology. Nine (25.7%) of 35 PDD/DLB cases with psyn immunoreactivity in the skin were complicated by AD pathology or Braak neurofibrillary tangle stage equal to or more than III and senile plaque stage equal to C (21). In contrast, 14 of 37 anti-psyn negative PDD/DLB cases (37.8%) were complicated by AD pathology (Table 5). Seven (20%) of 35 PDD/DLB cases with LB pathology of the skin were complicated by AGD stage II or greater. Twelve (32.4%) of 37 cases without LB pathology in the skin were complicated by AGD stage II or greater. Thus, AD pathology or high-grade AGD pathology complicated 14 (40%) of 35 psyn-positive cases and 25 (67.6%) of 37 psyn-negative cases. The rate of complication by AD and/or AGD pathology was significantly higher in PDD/DLB patients without dermal α-synucleinopathy than in PDD/DLB patients with accompanying LB-related pathology in the skin ($p = 0.019$; Table 5).

Clinicopathologic Correlation of Subclinical and Clinical LBD With LB Pathology in the Skin

Activities of daily living (ADL) data on the 84 patients without dermal LB-related pathology in the retrospective study were as follows: bedridden, 39 patients (46.4%); wheelchair-bound, 6 patients (7.1%); cane-assisted, 13 patients (15.5%); and walking independently, 26 patients (31.0%). The ADL data on the 58 patients with dermal LB-related pathology were as follows: bedridden, 37 patients (63.8%); wheelchair-bound, 7 patients (12.1%); cane-assisted, 4 patients (6.9%); and walking independently, 10 patients (17.2%). The proportion of bedridden patients was significantly higher ($p < 0.001$) and the proportion of patients walking independently tended to be lower ($p = 0.065$) among psyn-positive patients compared with psyn-negative patients. The numbers of bedridden patients with decubitus ulcers were as follows: dermal psyn-negative patients, 14 (35.6%) of 39; dermal psyn-positive patients, 21 (56.8%) of 37. Thus, patients with positive dermal LB pathology had a significantly higher rate of decubitus ulcers than dermal LB-negative patients ($p = 0.028$).

TABLE 4. Lewy Body Pathology in the Abdominal Skin in Subclinical and Clinical LBD

LB Stage	Subtype	n	Dermal LBD, %	Adrenal LB, %
II		56	13 (23.2)	42 (75)
	B	16	3 (18.8)	12 (75)
	T	34	9 (26.5)	26 (76.5)
	N	4	1 (25.0)	4 (100)
II	A	2	0	0
III		14	10 (71.4)	14 (100)
	B	9	6 (66.7)	9 (100)
	T	3	2 (66.7)	3 (100)
	N	2	2 (100)	2 (100)
IV		38	17 (44.7)	33 (100)
P	PDDT	13	8 (61.5)	13 (100)
D	DLBT	25	9 (36.0)	20 (80)
V		34	18 (52.9)	30 (88.2)
P	PDDN	7	6 (85.7)	7 (100)
D	DLBN	27	12 (44.4)	23 (85.2)

Differential diagnosis of PDD and DLB was based on the "1-year rule" in the consensus guidelines (19). Subtype was based on LB score: B, brainstem; T, transitional; and N, neocortical. A, Amygdala variant, represents LB pathology centered around amygdala and lacking involvement of the peripheral autonomic nervous system (2).

D, dementia with LBs; DLBN, dementia with LBs, with an LB score corresponding to the value for the neocortical form; DLBT, dementia with LBs, with an LB score corresponding to the value for the transitional form; LB, Lewy body; LBD, LB disease; P, PD with dementia; PD, Parkinson disease; PDDN, PD with dementia, with an LB score corresponding to the value for the neocortical form; PDDT, PD with dementia, with an LB score corresponding to the value for the transitional form.

TABLE 5. Influence of Coexistent Pathology in the Form of AD or AGD on LB Pathology Involving the Skin in Patients with PDD or DLB

		n	AD(+)	AGD(+)	Total*
Skin psyn(+)	Total	35	9 (25.7%)	7 (20%)	14 (40%)
	PDD	14	2	2	4
	DLB	21	7	5	10
Skin psyn(−)	Total	37	14 (37.8%)	12 (32.4%)	25 (67.6%)
	PDD	6	0	3	2
	DLB	31	14	10	23

*Number of cases complicated by either AD or AGD.

AD, Alzheimer disease; AGD, argyrophilic grain disease; DLB, dementia with LBs; PDD, Parkinson disease with dementia.

DISCUSSION

This study is the first to demonstrate that LB-related pathology involves the cutaneous nerves in LBD. Because LB-related pathology identified in the skin was only seen in cases that had LB-related pathology in the CNS and not in 194 cases without CNS LB-related pathology, there were no false-positives; the specificity is, therefore, 100%. The sensitivity of LB pathology in the skin was 70% in PD and 40% in DLB in single sampling from the abdominal surface. The PDD or DLB cases without LB-related pathology in the skin were more frequently complicated by AD or AGD pathology than were those with LB-related pathology in the skin.

Sympathetic nerve fibers innervate blood vessels, eccrine glands, and the erector pili muscles in the skin. Sympathetic nerve fibers that innervate eccrine glands are cholinergic nerves, whereas all others are adrenergic. The psyn-positive structures were colocalized with axons visualized with SMI31 in the skin and were associated with axons by electron microscopy and TH immunohistochemistry. In light of these findings, we speculate that the psyn immunoreactivity was localized in the adrenergic nerves that innervate blood vessels and erector pili muscles in the skin. Not all psyn immunoreactivities were colocalized with anti-TH-immunoreactive axons, however, and it is more probable that α-synuclein also accumulates in the cholinergic nerves that innervate eccrine glands.

By electron microscopy, classic perikaryonal and intraneuritic LBs in the CNS are composed of a dense central core and surrounded by radiating filaments and vesicles. The LBs in the axons consist of randomly arranged or aggregated filamentous material with an inner core composed of electron-dense granular material. Immunohistochemical studies with anti-psyn antibodies have demonstrated axonal swellings in the cerebral white matter (16); these axonal swellings

© 2008 American Association of Neuropathologists, Inc.

Copyright © 2008 by the American Association of Neuropathologists, Inc. Unauthorized reproduction of this article is prohibited.

contained mitochondria and dense and lamellated bodies ultrastructurally (data not shown). Our electron microscopic findings of psyn-immunoreactive structures in the skin seem to be similar to those of axonal swellings in the CNS. This suggests that the cutaneous nerves were directly affected by LB-type accumulation of psyn.

Tests such as the thermal sweat test, pilocarpine sweat test, and sympathetic skin response have been used clinically to evaluate sudomotor function. There have been some clinical reports of the use of these tests to gauge sudomotor function in PD, but the severity and distribution of sudomotor dysfunction differ between each study (24–26). Studies suggest that the central or preganglionic sympathetic fibers may be involved in the early-stage lesions responsible for sudomotor dysfunction; postganglionic sympathetic fibers may become involved with progression of the disease. There have been few pathological studies of the skin in LBD (27), and no reports have described LB-related pathology in the skin. Our studies provide definite morphological evidence of the involvement of postganglionic axon terminals in LBD.

There is controversy regarding the distribution of clinical sudomotor dysfunction in LBD. Most reports indicate that although sweating preferentially decreases in the distal extremities, the distribution of the sudomotor dysfunction is patchy and differs among patients. Our prospective studies of the brachial and abdominal skin showed that psyn immunoreactivity was not always the same in skin from 2 different anatomical locations. Because the distal extremities were frequently affected by ischemic changes in our elderly cohort, we chose a proximal extremity and the trunk for the evaluation of LBD pathology. If skin biopsy is to become a useful tool in the diagnosis of LBD, it will be necessary to choose an area of skin where physiological tests consistently show definite abnormalities. Low sensitivity (about 20%) of dermal LB pathology among subclinical LBD cases (our CNS LB stage II) may also indicate that random skin biopsy is not valid for the early diagnosis of LBDs.

We retrospectively investigated possible correlations between the patients' ADL and skin LB pathology and found that ADL criteria were worse in patients with positive LB-related pathology in the skin than in those without it. This result is consistent with the clinical consensus in LBD that autonomic dysfunction usually parallels motor signs. Moreover, dermal psyn-positive patients had a significantly higher rate of complications in the form of decubitus ulcers than did the negative patients. Although the main cause of decubitus ulceration relates to motor disturbance in LBD patients, the direct involvement of the skin by LBD may be a contributing factor that warrants additional attention.

Our results also reveal that the epitope of phosphorylated α-synuclein accumulates in the cutaneous nerves in subclinical LBD. This finding is consistent with cardiac 123I-metaiodobenzylguanidine scintigraphic finding of involvement of unmyelinated fibers in the epicardial fatty tissue in incidental LBD (28).

Dermal psyn immunoreactivity was observed most frequently in PD (without dementia) and reached 100% in the prospective study, although the number of cases was small. In CNS LB stages IV and V, LB-related pathology in the skin was more frequent in PDD than in DLB. In addition, PDD and DLB cases without cutaneous LB-related pathology were more frequently complicated by the pathology of AD or AGD. Braak et al (29) proposed a staging paradigm whereby LB-related pathology first occurs in the dorsal motor nucleus of the vagus nerve, extends rostrally in the brainstem, reaches the limbic system, and eventually affects the cerebral cortex. Cumulative evidence indicates that LB-related pathology preferentially localizes itself in the amygdala in AD (30) and other tauopathies (14); this pattern of distribution has been termed the *amygdala variant* (2). We previously found that the adrenal glands were always free of LB-related pathology in such cases of amygdala variant (2). Although in the present study the number of cases was small, the skin was always free of LB-related pathology in the cases of *amygdala variant* studied (Table 4). These data further support our hypothesis that the presence of other dementing pathology in the CNS, such as AD or AGD, may induce cerebrally predominant distribution of LB pathology with relative sparing of the PANS.

One of the 279 patients in the prospective study presented with many LB-related pathological features in the abdominal skin and LBs in the adrenal glands but only very few Lewy neurites and dots in the dorsal motor nucleus of the vagus in the CNS. This case might represent the earliest stage of LBPAF.

For the differential diagnosis among parkinsonian syndromes, we additionally examined 3 more cases with MSA (2 MSA-P and 1 MSA-C patients) since 2006 and confirmed negative results. Although more cases should be analyzed for further confirmation and assessment of specificity, anti-psyn immunoreactivity of the skin was only positive for LBD and negative for MSA, progressive supranuclear palsy, and corticobasal degeneration in this study.

In conclusion, we document LB-related pathology involvement in cutaneous nerves in LBD. Skin biopsy may, therefore, have diagnostic application in cases of PD or LBPAF with advanced autonomic failure.

ACKNOWLEDGMENTS

The authors thank Mr Naoo Aikyo, Ms Mieko Harada, Mr Satoru Fukuda, and Ms Nobuko Naoi (Department of Neuropathology, Tokyo Metropolitan Institute for Gerontology) for the preparation of sections and Dr Kinuko Suzuki for helpful discussions. We also thank 2 anonymous neurologists for preparing the Clinical Dementia Rating scale used in this study.

REFERENCES

1. Kosaka K, Yoshimura M, Ikeda K, et al. Diffuse type of Lewy body disease: Progressive dementia with abundant cortical Lewy bodies and senile changes of varying degree—a new disease? Clin Neuropathol 1984;3:185–92
2. Fumimura Y, Ikemura M, Saito Y, et al. Analysis of the adrenal gland is useful for evaluating pathology of the peripheral autonomic nervous system in Lewy body disease. J Neuropathol Exp Neurol 2007;66: 354–62
3. Wakabayashi K, Takahashi H, Takeda S, et al. Parkinson's disease: The presence of Lewy bodies in Auerbach's and Meissner's plexuses. Acta Neuropathol (Berl) 1988;76:217–21
4. Wakabayashi K, Takahashi H, Ohama E, et al. Parkinson's disease: An

© 2008 American Association of Neuropathologists, Inc.

Copyright © 2008 by the American Association of Neuropathologists, Inc. Unauthorized reproduction of this article is prohibited.

immunohistochemical study of Lewy body–containing neurons in the enteric nervous system. Acta Neuropathol (Berl) 1990;79:581–83
5. Qualman SJ, Haupt HM, Yang P, et al. Esophageal Lewy bodies associated with ganglion cell loss in achalasia. Gastroenterology 1984; 87:848–56
6. Wakabayashi K, Takahashi H. Neuropathology of autonomic nervous system in Parkinson's disease. Eur Neurol 1997;38(Suppl 2):2–7
7. Wakabayashi K. Parkinson's disease: The distribution of Lewy bodies in the peripheral autonomic nervous system. No To Shinkei 1989;41:965–71
8. Den Hartog Jager WA, Bethlem J. The distribution of Lewy bodies in the central and autonomic nervous systems in idiopathic paralysis agitans. J Neurol Neurosurg Psych 1960;23:283–90
9. Orimo S, Oka T, Miura H, et al. Sympathetic cardiac denervation in Parkinson's disease and pure autonomic failure but not in multiple system atrophy. J Neurol Neurosurg Psych 2002;73:776–77
10. Orimo S, Ozawa E, Nakade S, et al. (123)I-metaiodobenzylguanidine myocardial scintigraphy in Parkinson's disease. J Neurol Neurosurg Psych 1999;67:189–94
11. Mitsui J, Saito Y, Momose T, et al. Pathology of the sympathetic nervous system corresponding to the decreased cardiac uptake in 123I-metaiodobenzylguanidine (MIBG) scintigraphy in a patient with Parkinson disease. J Neurol Sci 2006;243:101–4
12. Forno LS, Norville RL. Ultrastructure of Lewy bodies in the stellate ganglion. Acta Neuropathol (Berl) 1976;34:183–97
13. Saito Y, Ruberu NN, Sawabe M, et al. Staging of argyrophilic grains: An age-associated tauopathy. J Neuropathol Exp Neurol 2004;63: 911–18
14. Saito Y, Ruberu NN, Sawabe M, et al. Lewy body-related a-synucleinopathy in aging. J Neuropathol Exp Neurol 2004;63:742–49
15. Saito Y, Nakahara K, Yamanouchi H, et al. Severe involvement of ambient gyrus in dementia with grains. J Neuropathol Exp Neurol 2002; 61:789–96
16. Saito Y, Kawashima A, Ruberu NN, et al. Accumulation of phosphorylated alpha-synuclein in aging human brain. J Neuropathol Exp Neurol 2003;62:644–54
17. Fujiwara H, Hasegawa M, Dohmae N, et al. a-Synuclein is phosphorylated in synucleinopathy lesions. Nat Cell Biol 2002;4:160–64
18. McKeith IG, Dickson DW, Lowe J, et al. Diagnosis and management of dementia with Lewy bodies: Third report of the DLB Consortium. Neurology 2005;65:1863–72
19. McKeith IG, Galasko D, Kosaka K, et al. Consensus guidelines for the clinical and pathologic diagnosis of dementia with Lewy bodies (DLB): Report of the Consortium on DLB international workshop. Neurology 1996;47:1113–24
20. Braak H, Braak E. Neuropathological staging of Alzheimer-related changes. Acta Neuropathol (Berl) 1991;82:239–59
21. Murayama S, Saito Y. Neuropathological diagnostic criteria for Alzheimer's disease. Neuropathology 2004;24:254–60
22. Jellinger KA. Dementia with grains (argyrophilic grain disease). Brain Pathol 1998;8:377–86
23. Jellinger KA, Bancher C. Senile dementia with tangles (tangle predominant form of senile dementia). Brain Pathol 1998;8:367–76
24. Kihara M, Kihara Y, Tukamoto T, et al. Assessment of sudomotor dysfunction in early Parkinson's disease. Eur Neurol 1993;33:363–65
25. Mano Y, Nakamuro T, Takayanagi T, et al. Sweat function in Parkinson's disease. J Neurol 1994;241:573–76
26. Turkka JT, Myllyla VV. Sweating dysfunction in Parkinson's disease. Eur Neurol 1987;26:1–7
27. Dabby R, Djaldetti R, Shahmurov M, et al. Skin biopsy for assessment of autonomic denervation in Parkinson's disease. J Neural Transm 2006; 113:1169–76
28. Orimo S, Takahashi A, Uchihara T, et al. Degeneration of cardiac sympathetic nerve begins in the early disease process of Parkinson's disease. Brain Pathol 2007;17:24–30
29. Braak H, Del Tredici K, Rub U, et al. Staging of brain pathology related to sporadic Parkinson's disease. Neurobiol Aging 2003;24:197–211
30. Lippa CF, Fujiwara H, Mann DM, et al. Lewy bodies contain altered a-synuclein in brains of many familial Alzheimer's disease patients with mutations in presenilin and amyloid precursor protein genes. Am J Pathol 1998;153:1365–70

© 2008 American Association of Neuropathologists, Inc.

Copyright © 2008 by the American Association of Neuropathologists, Inc. Unauthorized reproduction of this article is prohibited.

ORIGINAL CONTRIBUTION

Development of a High-Throughput Microarray-Based Resequencing System for Neurological Disorders and Its Application to Molecular Genetics of Amyotrophic Lateral Sclerosis

Yuji Takahashi, MD, PhD; Naomi Seki, MD, PhD; Hiroyuki Ishiura, MD; Jun Mitsui, MD; Takashi Matsukawa, MD; Atsushi Kishino, MD; Osamu Onodera, MD, PhD; Masashi Aoki, MD, PhD; Nobuyuki Shimozawa, MD, PhD; Shigeo Murayama, MD, PhD; Yasuto Itoyama, MD, PhD; Yasuyuki Suzuki, MD, PhD; Gen Sobue, MD, PhD; Masatoyo Nishizawa, MD, PhD; Jun Goto, MD, PhD; Shoji Tsuji, MD, PhD

Background: Comprehensive resequencing of the causative and disease-related genes of neurodegenerative diseases is expected to enable (1) comprehensive mutational analysis of familial cases, (2) identification of sporadic cases with de novo or low-penetrant mutations, (3) identification of rare variants conferring disease susceptibility, and ultimately (4) better understanding of the molecular basis of these diseases.

Objective: To develop a microarray-based high-throughput resequencing system for the causative and disease-related genes of amyotrophic lateral sclerosis (ALS) and other neurodegenerative diseases.

Design: Validation of the system was conducted in terms of the signal-to-noise ratio, accuracy, and throughput. Comprehensive gene analysis was applied for patients with ALS.

Subjects: Ten patients with familial ALS, 35 patients with sporadic ALS, and 238 controls.

Results: The system detected point mutations with 100% accuracy and completed the resequencing of 270 kilobase pairs in 3 working days with greater than 99.9% accuracy of base calls, or the determination of base(s) at each position. Analysis of patients with familial ALS revealed 2 *SOD1* mutations. Analysis of the 35 patients with sporadic ALS revealed a previously known *SOD1* mutation, S134N, a novel putative pathogenic *DCTN1* mutation, R997W, and 9 novel variants including 4 nonsynonymous heterozygous variants consisting of 2 in *ALS2*, 1 in *ANG*, and 1 in *VEGF* that were not found in the controls.

Conclusion: The DNA microarray–based resequencing system is a powerful tool for high-throughput comprehensive analysis of causative and disease-related genes. It can be used to detect mutations in familial and sporadic cases and to identify numerous novel variants potentially associated with genetic risks.

Arch Neurol. 2008;65(10):1326-1332

Author Affiliations are listed at the end of this article.

With recent progress in human molecular genetics, many causative genes of inherited neurological diseases have been identified. In 2007, 667 neurological diseases were registered in the Online Mendelian Inheritance in Man database (http://www.ncbi.nlm.nih.gov/entrez/query.fcgi?db=OMIM) as diseases with identified causative genes. It should be noted that there are substantial nonallelic genetic heterogeneities in hereditary neurodegenerative diseases, including amyotrophic lateral sclerosis (ALS), Parkinson disease, Alzheimer disease, and hereditary spastic paraplegia. Thus, there is a strong demand for comprehensive mutational analysis of multiple causative genes in daily clinical practice.

Most neurodegenerative diseases are sporadic and their molecular etiologies remain unknown. Although genome-wide association studies (GWAS) using common variants of single nucleotide polymorphisms have been undertaken to identify the loci of disease-susceptibility genes, genetic risks associated with rare variants may not be captured by GWAS.[1] Identification of multiple rare variants, however, would need comprehensive resequencing of candidate genes. Furthermore, sporadic diseases may be caused by de novo mutations or low-penetrant mutations in the causative genes. Taken together, development of a comprehensive resequencing system of causative genes will be indispensable, not only to provide mutational analyses of multiple causative genes for familial diseases, but also to explore the molecular basis of sporadic diseases.

©2008 American Medical Association. All rights reserved.